Computational and Structural Biotechnology Journal 18 (2020) 2596–2609

COMPUTATIONAL AND STRUCTURAL BIOTECHNOLOGY JOURNAL

journal homepage: www.elsevier.com/locate/csbj

A metagenome-wide association study of gut microbiome and visceral fat accumulation

Xiaomin Nie [a,1], Jiarui Chen [b,c,1], Xiaojing Ma [a], Yueqiong Ni [b], Yun Shen [a], Haoyong Yu [a,*], Gianni Panagiotou [b,c,d,*], Yuqian Bao [a,*]

[a] Department of Endocrinology and Metabolism, Shanghai Jiao Tong University Affiliated Sixth People's Hospital, Shanghai Clinical Center for Diabetes, Shanghai Key Clinical Center for Metabolic Disease, Shanghai Diabetes Institute, Shanghai Key Laboratory of Diabetes Mellitus, Shanghai 200233, China
[b] Leibniz Institute for Natural Product Research and Infection Biology – Systems Biology and Bioinformatics, Hans Knöll Institute, Adolf-Reichwein-Straße 23, 07745 Jena, Germany
[c] School of Biological Sciences, The University of Hong Kong, Kadoorie Biological Sciences Building, Pok Fu Lam Road, Hong Kong Special Administrative Region
[d] Department of Medicine and State Key Laboratory of Pharmaceutical Biotechnology, The University of Hong Kong, Hong Kong Special Administrative Region

ARTICLE INFO

Article history:
Received 17 June 2020
Received in revised form 3 September 2020
Accepted 15 September 2020
Available online 20 September 2020

Keywords:
Gut microbiome
Obesity
Visceral fat
Laparoscopic sleeve gastrectomy
Metagenomics

ABSTRACT

Purpose: Visceral fat is an independent risk factor for metabolic and cardiovascular disease. The study aimed to investigate the associations between gut microbiome and visceral fat.
Methods: We recruited 32 obese adults and 30 healthy controls at baseline. Among the obese subjects, 14 subjects underwent laparoscopic sleeve gastrectomy (LSG) and were followed 6 months after surgery. Abdominal visceral fat area (VFA) and subcutaneous fat area (SFA) were measured by magnetic resonance imaging. Waist, hipline, waist-to-hip ratio (WHR) and body mass index (BMI) were included as simple obese parameters. Gut microbiome was analyzed by metagenomic sequencing.
Results: Among the obese parameters, VFA had the largest number of correlations with the species that were differentially enriched between obese and healthy subjects, following by waist, WHR, BMI, hipline, and SFA. Within the species negatively correlated with VFA, *Eubacterium eligens* had the strongest correlation, following by *Clostridium citroniae*, *C. symbiosum*, *Bacteroides uniformis*, *E. ventriosum*, *Ruminococcaceae bacterium D16*, *C. hathewayi*, etc. *C. hathewayi* and *C. citroniae* were increased after LSG. Functional analyses showed that among all the obese parameters, VFA had strongest correlation coefficients with the obesity-related microbial pathways. Microbial pathways involved in carbohydrate fermentation and biosynthesis of L-glutamate and L-glutamine might contribute to visceral fat accumulation.
Conclusions: Visceral fat was more closely correlated with gut microbiome compared with subcutaneous fat, suggesting an intrinsic connection between gut microbiome and metabolic cardiovascular diseases. Specific microbial species and pathways which were closely associated with visceral fat accumulation might contribute to new targeted therapies for metabolic disorders.

Abbreviations: 2hCP, 2-hour C-peptide; 2hPG, 2-hour plasma glucose; ALT, alanine aminotransferase; AST, aspartate aminotransferase; BCAAs, branched chain amino acids; BMI, body mass index; CoDA, Compositional Data Analysis; Cr, creatinine; DBP, diastolic blood pressure; FCp, fasting C-peptide; FDR, false discovery rate; FMT, fecal microbiota transplantation; FPG, fasting plasma glucose; GPR43, G-protein coupled receptor 43; HbA1c, glycated hemoglobin A1c; HDL, high-density lipoprotein cholesterol; LDL, low-density lipoprotein cholesterol; LPS, lipopolysaccharides; LSG, laparoscopic sleeve gastrectomy; MRI, magnetic resonance imaging; MSG, monosodium glutamate; SBP, systolic blood pressure; SCFAs, short chain fatty acids; SFA, subcutaneous fat area; TC, total cholesterol; TCA, tricarboxylic acid cycle; TG, triglyceride; UA, uric acid; VFA, visceral fat area; WBC, white blood cell count; WHR, waist-to-hip ratio.

* Corresponding authors at: Department of Endocrinology and Metabolism, Shanghai Jiao Tong University Affiliated Sixth People's Hospital, 600 Yishan Road, Shanghai 200233, China (H. Yu and Y. Bao). Leibniz Institute for Natural Product Research and Infection Biology – Systems Biology and Bioinformatics, Hans Knöll Institute, Adolf-Reichwein-Straße 23, 07745 Jena, Germany (G. Panagiotou).

E-mail addresses: yuhaoyong111@163.com (H. Yu), Gianni.Panagiotou@hki-jena.de (G. Panagiotou), yqbao@sjtu.edu.cn (Y. Bao).

[1] These two authors contributed equally to this work.

https://doi.org/10.1016/j.csbj.2020.09.026

1. Introduction

About 10^{14} microbes live in the human gut [1]. This complex and dynamic ecosystem functions like an organ, profoundly influencing its host's energy metabolism and immunoregulation. The pivotal role of gut microbiota in obesity has now been widely recognized [2–4]. Using polymerase chain reaction, gene chip technology, and 16S rRNA sequencing, previous studies have linked the composition of gut microbiota with obesity [5–7]. Fecal microbiota transplantation (FMT) and germ-free mouse model establish causality for these correlations [8–10]. Compared with 16S rRNA sequencing, metagenomic sequencing provides information on gut microbes at the species or even strains level. Some bacteria, such as *Bacteroides thetaiotaomicron*, *Akkermansia muciniphila* and *Lactobacillus reuteri* are protective against obesity and diabetes [11–13]. Functional analyses based on metagenomic sequencing describe the complex and diverse functions of gut microbiota [14]. Some microbial metabolites such as lipopolysaccharides (LPS), short chain fatty acids (SCFAs) and branched chain amino acids (BCAAs) and bile acids metabolism were involved in the correlation mechanisms of gut microbiota and energy metabolism [11,15–18].

The pathogenesis and progression of the obesity-related cardiometabolic complications are primarily dependent on fat distribution [19]. Visceral fat and subcutaneous fat are significantly different even from an ontogenetic sight [20]. Visceral fat accumulation significantly increases the risks of type 2 diabetes [21], cardiovascular disease [22], cancer [23], and all-cause mortality [24]; whereas subcutaneous fat acts as a "buffer pool" for the circulating fatty free acid and has a protective role in metabolism [25]. Nevertheless, few studies have investigated the relationship between visceral fat and gut microbiota. These previous studies explored the role of gut microbiome only to the phylum or genus level [26–28]. Bacterial species belonging to the same genus sometimes have distinct functions. For example, *B. thetaiotaomicron* ameliorates colon inflammation in preclinical models of Crohn's disease [29], while *B. pyogenes* causes bacteremia secondary to liver abscess [30]. In order to reduce complications in FMT and find potential therapeutic targets, it is essential to discover the contributions of specific bacterial species to the disease phenotype. In this study, we aimed to investigate the relationships between gut microbiome and visceral fat accumulation in a cross-sectional cohort, and further explore the changes of the visceral fat-associated bacterial species in a longitudinal cohort after weight loss intervention.

2. Results

2.1. Clinical characteristics of subjects

The study included a cross-sectional cohort with 32 obese adults and 30 healthy participants and a longitudinal cohort with 14 of the obese subjects receiving laparoscopic sleeve gastrectomy (LSG) who were followed 6 months after surgery (Fig. 1a). Visceral fat area (VFA) and subcutaneous fat area (SFA) were precisely measured by magnetic resonance imaging (MRI) for all participants. VFA and SFA had opposite correlations with the parameters of glycolipid metabolism (Fig. 1b). VFA and waist-to-hip ratio (WHR) was positively correlated with the inferior glycolipid parameters, while SFA and hipline seemed to be protective on glucose metabolism (Fig. 1b). Compared with healthy controls, obese subjects had significantly higher obese parameters and worse homeostasis in glucose metabolism, lipid metabolism, hepatic function, uric acid (UA) and systemic inflammation (Wilcoxon rank sum test; $p < 0.05$; Fig. 1c; Suppl. Table 1). At 6 months after LSG, almost all the obese parameters (except for WHR) experienced significant decrease, with median values decreased by 8.39 kg/m^2 for body mass index (BMI), 89.95 cm^2 for VFA, and 216.80 cm^2 for SFA (Fig. 1c). Compared with the pre-operative status, blood pressure, glucose metabolism, lipid metabolism, hepatic function, and inflammation significantly improved 6 months after LSG (paired-sample Wilcoxon test; $p < 0.05$; Suppl. Table 1).

2.2. Community diversity in obese adults, healthy controls and after LSG

Community diversity including alpha and beta diversity were evaluated at taxonomic levels from phylum to family, genus, and species. Alpha diversity by Shannon index was not significantly different between healthy controls and obese subjects at all taxonomic levels (Fig. 2a). However, alpha diversity of post-operative communities was significantly increased at the species level compared with pre-operative communities (paired Wilcoxon signed-rank test; $p < 0.05$) (Fig. 2a).

We subsequently investigated community dissimilarity among participant groups based on beta diversity by Bray-Curtis index and Aitchison distance. Comparisons of the Bray-Curtis distance between healthy and obese samples showed no significant separation by nonmetric dimensional scaling ordination (permutational multivariate analysis of variance (PERMANOVA); $p = 0.42$) (Fig. 2b). However, within-group distances were significantly higher in obese subjects than in healthy controls, suggesting the microbiome communities were more similar within the population of healthy participants (Wilcoxon rank sum test; $p < 0.05$) (Fig. 2c). Furthermore, comparisons of the Aitchison distance between healthy and obese subjects suggested a significant separation (PERMANOVA; $p < 0.05$) (Suppl. Fig. 4a). The significantly higher within-group distances in obese patients comparing with healthy subjects consistently proposed the higher variations within the obese population (Wilcoxon rank sum test; $p < 0.05$) (Suppl. Fig. 4b). We further observed significant differences in Bray-Curtis distance between pre- vs. post-operative subjects (PERMANOVA; $p < 0.05$) (Fig. 2d) with within-group distances significantly decreased after LSG (Wilcoxon rank sum test; $p < 0.05$) (Fig. 2e). However, from the view of Aitchison distance, the difference between pre- and post-operative subjects lost the significance but still with the same trends (PERMANOVA; $p = 0.14$; Wilcoxon rank sum test; $p = 0.34$) (Suppl. Fig. 4c & d). Furthermore, by comparing between-group distances, we observed that healthy controls and post-operative subjects had significantly lower Bray-Curtis distances (Wilcoxon rank sum test; $p < 0.05$) (Fig. 2f). The significant differences in between-group Bray-Curtis diversity among participants who were healthy, obese, pre- or post-operative suggested that the LSG made the overall microbial community of obese subjects more similar with a healthy community.

2.3. Association among gut microbiome profiles, obesity and LSG

2.3.1. Microbial differences from comparisons of healthy controls vs. obese subjects and pre- vs. post-operative subjects

We compared microbial differences at the species level between healthy controls and obese subjects (Suppl. Table 2). We identified 20 different species (Wilcoxon rank sum test; original $p < 0.05$; $q < 0.37$) (Fig. 3a), with 14 enriched in healthy controls and 6 enriched in obese subjects. A group of species belonging to order *Clostridiales* (such as *Eubacterium eligens*, *Clostridium citroniae*, *C. hathewayi*, and *C. symbiosum*) were enriched in healthy controls. Three species belonging to order *Bacteroidales* (*Paraprevotella xylaniphila*, *Alistipes shahii*, and *B. uniformis*) were also enriched in healthy controls. *B. massiliensis*, *Escherichia coli*, *Dorea longicatena*, *E. hallii*, *Slackia piriformis*, and *Eggerthella lenta* were enriched in

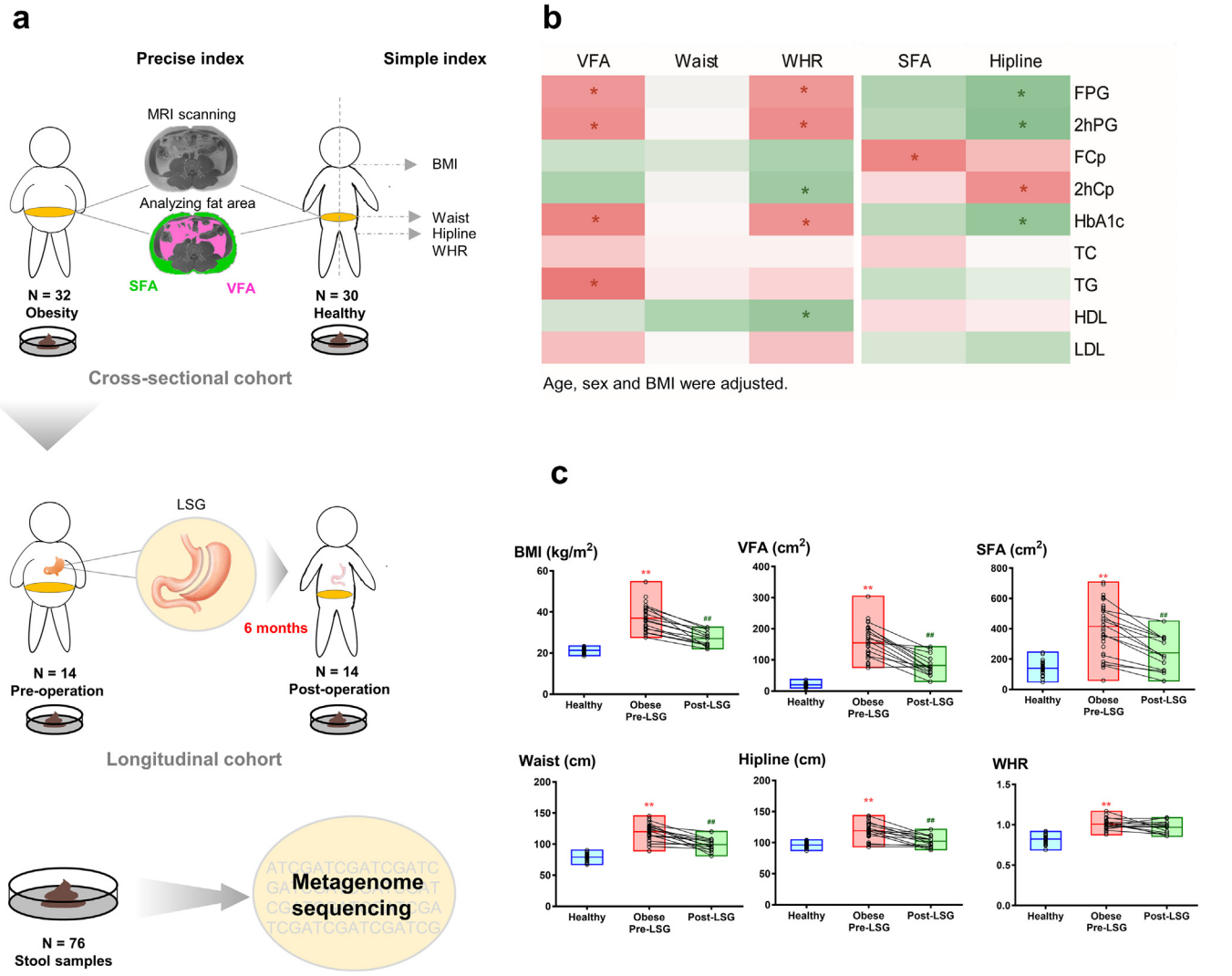

Fig. 1. Study design and characteristics of the obese parameters. (a) Study design including cross-sectional cohort and longitudinal cohort. (b) Partial correlation analysis between the obese parameters and metabolic parameters of glucose and lipid. Age, sex, and BMI were adjusted. Red columns indicated to positive correlations, green columns indicated to negative correlations, and * indicated to $p < 0.05$. (c) Comparisons of the obese parameters between healthy vs. obese subjects, pre- and post-operative subjects. ** indicated to $p < 0.01$ compared with healthy subjects; ## indicated to $p < 0.01$ compared with pre-operative subjects. (For interpretation of the references to color in this figure legend, the reader is referred to the web version of this article.)

obese subjects. We further evaluated the significant results by performing Compositional Data Analysis (CoDA). Among the 20 significantly different species, 10 species remained significant (Wilcoxon rank sum test; original $p < 0.05$; $q < 0.37$) (Fig. 3a).

After false discovery rate (FDR) correction, the healthy enrichment of *B. uniformis*, *E. eligens*, *Flavonifractor plautii*, *Ruminococcaceae bacterium D16*, *C. citroniae*, and *C. symbiosum* remained significant while the obese enrichment of *E. hallii* remained significant (Wilcoxon rank sum test; $q < 0.25$).

Species abundance was also compared for pre- and post-operative samples (Suppl. Table 2). We found 26 different species (paired Wilcoxon signed-rank test; original $p < 0.05$, $q < 0.28$) (Fig. 3b), within which 24 were enriched in post-operative group and 2 were enriched in pre-operative group. After FDR correction, we still observed 13 significantly different species, such as post-operative enrichment of *C. symbiosum, C. hathewayi*, *C. asparagiforme*, *Clostridiales bacterium 1 7 47FAA*, *Anaerotruncus colihominis*, *A. putredinis*, *C. bolteae*, *C. nexile*, *B. caccae*, *C. citroniae* and *B. thetaiotaomicron* (paired Wilcoxon signed-rank test; $q < 0.20$). Confirmed by CoDA, 8 species consistently showed significant difference (paired Wilcoxon signed-rank test; original $p < 0.05$; $q < 0.19$).

Combining results from comparisons of healthy controls vs. obese subjects and pre- vs. post-operative subjects showed 6 potentially beneficial species (*A. shahii*, *E. eligens*, unclassified *Oscillibacter*, *C. hathewayi*, *C. symbiosum* and *C. citroniae*) and 1 potentially harmful species (*D. longicatena*). The 6 beneficial species were all enriched in healthy controls, decreased in obese subjects, and increased to similar levels with healthy controls after LSG. Moreover, supported by the results from CoDA, the difference of *D. longicatena* and *C. symbiosum* in both comparisons remained significant (Fig. 3c).

2.3.2. Gut microbiome correlated with a panel of clinical characteristics

Spearman's correlation analysis was used to explore the correlations between species abundances and the clinical characteristics. Sixty-two samples combined from healthy controls and obese subjects were included. We found 271 correlations with original p values < 0.05 (Spearman's correlation value > 0.25 or < -0.25; $q < 0.61$) (Suppl. Table 3; Fig. 3d). Among the 6 obese parameters, VFA had the largest number of correlations with bacterial species (n = 26, $q < 0.08$), followed by waist (n = 24,

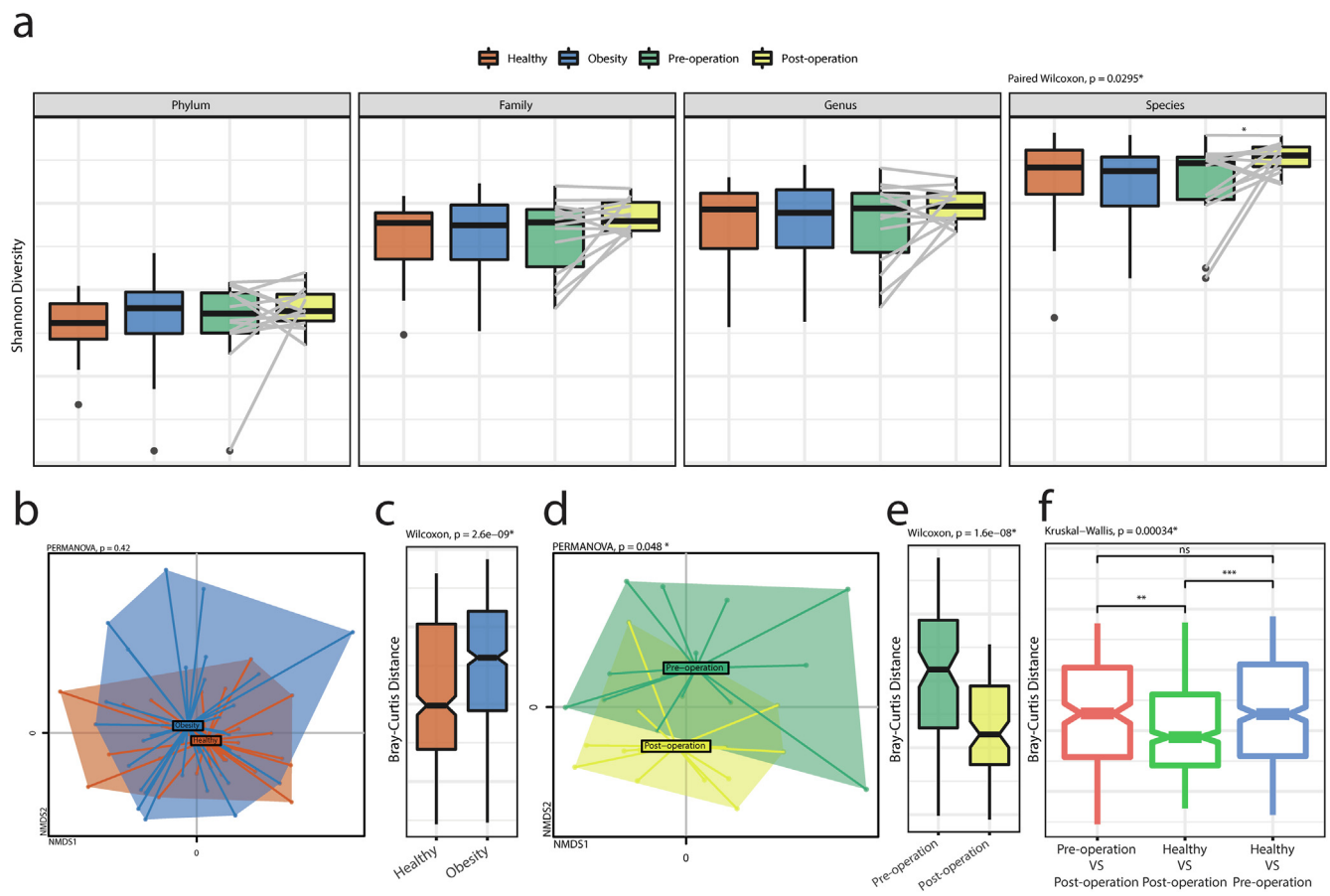

Fig. 2. Comparison of the microbial community among participant groups. (a) Alpha diversity of the four groups (healthy controls, obese subjects, pre-operative, and post-operative subjects) were analyzed at the phylum, family, genus, and species levels. Gray lines connected pairwise data of pre- and post-operative samples. (b) Non-metric multidimensional scaling (NMDS) plot of Bray-Curtis distances for healthy controls and obese subjects. (c) Within-group Bray-Curtis distance comparison for healthy controls and obese subjects. (d) NMDS plot based on Bray-Curtis distances for pre- and post-operative subjects. (e) Within-group Bray-Curtis distance comparisons for pre- and post-operative subjects. (f) Between-group Bray-Curtis distance comparisons among healthy controls, obese subjects, and post-operative subjects.

q < 0.09), waist-to-hip ratio (WHR, n = 20, q < 0.11), BMI (n = 18, q < 0.12), hipline (n = 14, q < 0.15) and SFA (n = 11, q < 0.19). *C. citroniae*, *C. symbiosum* and *E. eligens* had the most frequent correlations with the obese parameters (Fig. 3e). Within the species negatively correlated with VFA, *E. eligens* had the strongest correlation, followed by *C. citroniae*, *C. symbiosum*, *B. uniformis*, *E. ventriosum*, *Ruminococcaceae bacterium D16*, *C. hathewayi*, *A. shahii*, and *F. plautii*. Species negatively correlated with the obese parameters were also frequently and negatively correlated with triglyceride (TG), white blood cell count (WBC), low-density lipoprotein cholesterol (LDL), glycated hemoglobin A1c (HbA1c), fasting C-peptide (FCp), alanine aminotransferase (ALT), systolic blood pressure (SBP), and diastolic blood pressure (DBP), while were positively correlated with high-density lipoprotein cholesterol (HDL).

2.4. Co-abundance networks of species community

For a better understanding of the relationships among species and overall interconnectivity within individual communities, we evaluated the correlations among gut microbes with co-abundance networks based on the relative abundance of bacterial species. Networks were constructed using BAnOCC for four groups: healthy, obese, pre-, and post-operative (Fig. 4). Only significant edges with 95% credibility were used for network construction. Overall, co-occurrence relationships were within and between phylum *Actinobacteria*, *Bacteroidetes*, *Firmicutes*, *Fusobacteria* and *Proteobacteria*.

For healthy participants, networks showed 35 positive correlations and 12 negative correlations among 47 species (Fig. 4a). For obese participants, the number of significant correlations was more than twice as that of healthy participants, with 67 positive and 42 negative correlations among 49 species (Fig. 4b). The number of pre-operative correlations (86 positive, 29 negative) (Fig. 4c) was higher than that of post-operative correlations (61 positive, 36 negative) (Fig. 4d). We also tested differences in node centrality measures of node degree, betweenness, and closeness. Comparisons of healthy vs. obese groups and pre- vs. post-operative subjects using pairwise Wilcoxon signed-rank tests showed significantly higher node centrality in obese and pre-operative groups, respectively (node degree and node closeness between healthy and obese; node closeness between pre- vs. post-operative subjects; p < 0.05.) (Suppl. Fig. 1), suggesting higher centralization among species in these communities.

Comparisons of detailed co-occurrence results among groups (Suppl. Table 4) showed that positive correlations between *Megamonas hypermegale* and unclassified *Megamonas*, and between *Megamonas rupellensis* and unclassified *Meganomas* were consistently significant for all four groups. Correlations between *B. plebeius* and *B. coprocola*; unclassified *Citrobacter* and *Citrobacter freundii*; and unclassified *Veillonella* and *Veillonella parvula* were significant only in healthy controls and post-operative subjects, suggesting obesity might disrupt these correlations, which were then re-established after LSG.

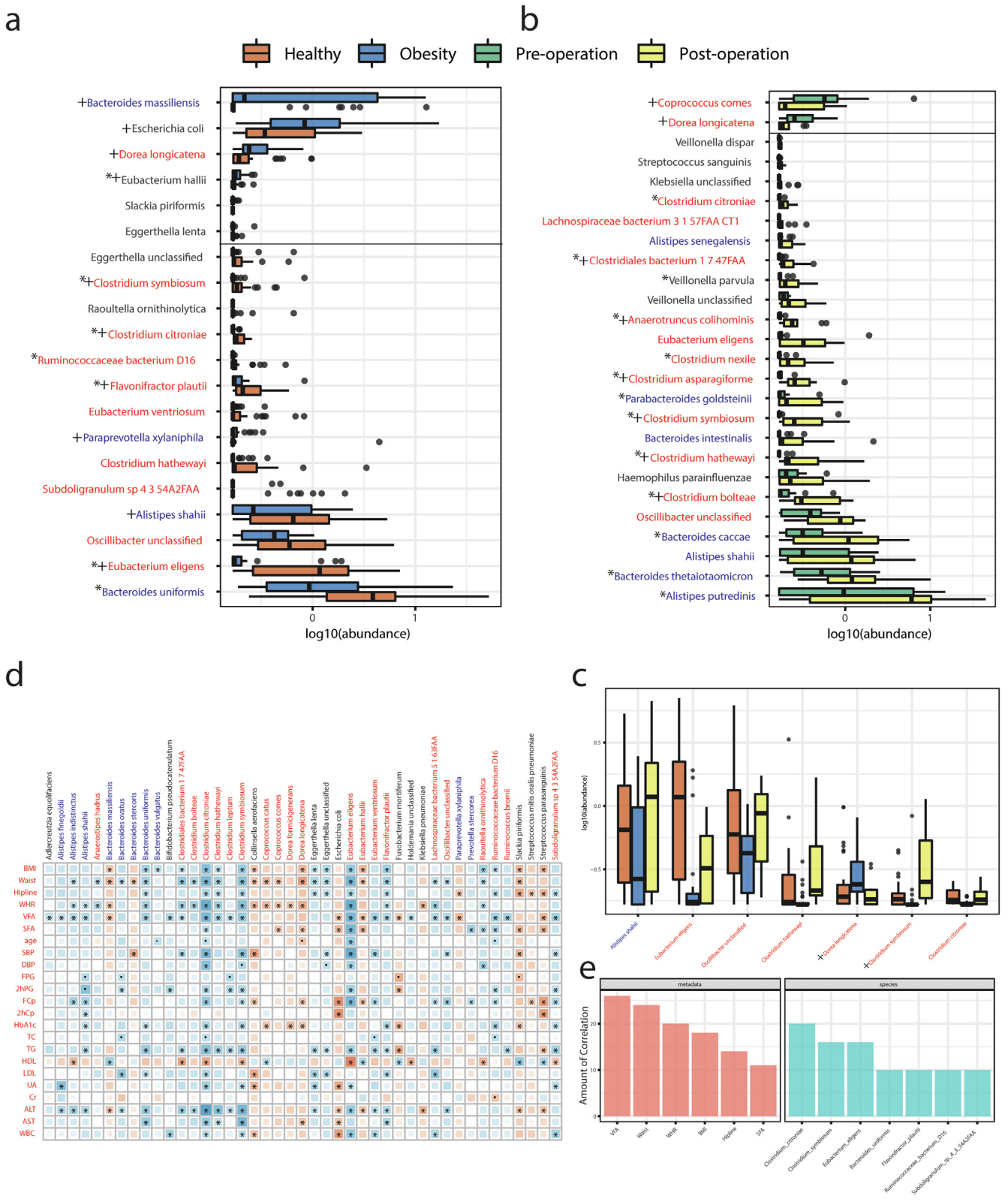

Fig. 3. Microbiome differences among groups and connections to obese parameters. (a) Abundance of species that were different between healthy controls and obese subjects. (b) Abundance of species that were significantly different in pre- and post-operative subjects. For (a), and (b), significant results after FDR correction were marked with stars. (c) Common species that differed in both comparisons. For (a), (b), and (c), significant results from CoDA were marked with the plus sign. (d) Correlation matrix for species and obese parameters. Cells in red indicated positive correlations while blue represented negative. Cell with dot indicated original $p < 0.05$, cells with star indicated $q < 0.25$. For (a), (b), (c), and (d), species from order *Clostridiales* were in red and from order *Bacteroidales* were in blue. (e) The amount of significant correlations for the six obese parameters and seven species with the most frequent correlations. (For interpretation of the references to color in this figure legend, the reader is referred to the web version of this article.)

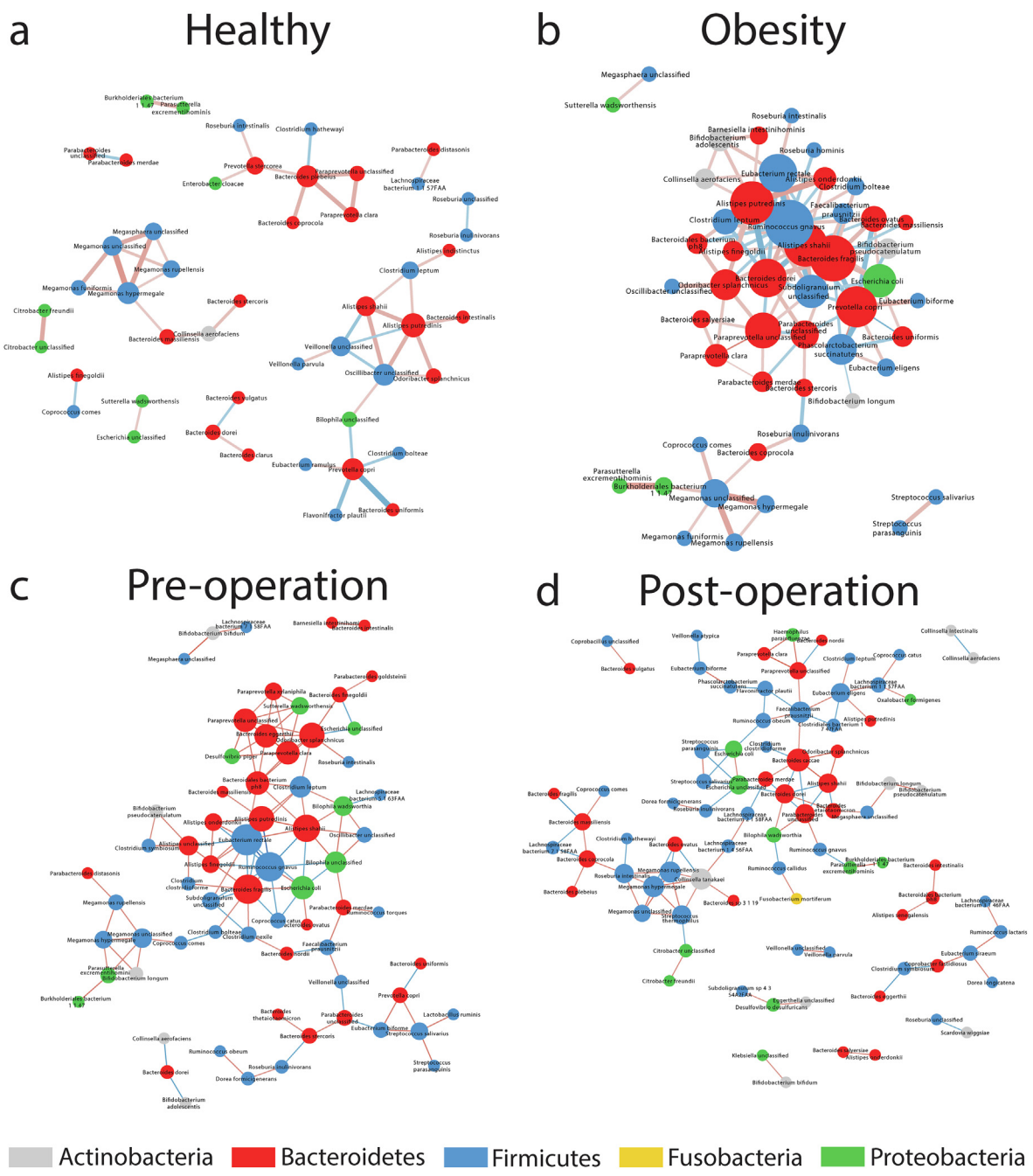

Fig. 4. Co-abundance relationships of communities. (a–d) Co-abundance networks for microbiome communities of (a) healthy controls, (b) obese subjects, (c) pre-, and (d) post-operative subjects. Only significant edges (based on 95% credibility interval) with |r| >= 0·3 (a, b) or 0·6 (c, d) were shown. Species from different phyla were marked with different colors (red circles: *Bacteroidetes*; green circles: *Proteobacteria*; blue circles: *Firmicutes*; grey circles: *Actinobacteria*; yellow circles: *Fusobacteria*). Blue edge, negative correlation; red edge, positive correlation. (For interpretation of the references to color in this figure legend, the reader is referred to the web version of this article.)

2.5. Functional shifts contributed by microbiome in different participants

2.5.1. Functional differences from comparisons of healthy controls vs. obese subjects and pre- vs. post-operative subjects

We also constructed functional profiles for each sample using the MetaCyc pathway database by HUMAnN2. We retrieved 330 microbial MetaCyc pathways. We evaluated functional alpha diversity by Shannon index which did not show significant differences either between healthy controls vs. obese subjects or pre- vs. post-operative subjects (Suppl. Fig. 2).

In the comparison of MetaCyc pathway abundance between healthy controls and obese subjects, 52 pathways were significantly different (Wilcoxon rank sum test; original $p < 0.05$, $q < 0.30$) (Fig. 5a; Suppl. Table 5). The two healthy-enriched pathways were: (1) glycolysis III (from glucose), a major pathway of central metabolism; and (2) GDP-mannose biosynthesis, a key substrate in glycoprotein formation. Within the 50 obesity-enriched pathways, 10 were responsible for energy generation (tricarboxylic acid cycle, TCA) and carbohydrate degradation, utilization and assimilation (fucose, rhamnose, glucose, D-glucarate, and glucose-1-phosphate); 14 were related to the biosynthesis of

cofactors, electron carriers and vitamins such as nicotinamide adenine dinucleotide, thiamine diphosphate, demethylmenaquinol and ubiquinol (these pathways contributed largely to redox reaction and TCA); 2 were involved in the biosynthesis of tetrahydrofolate. Two pathways involved in the biosynthesis of L-phenylalanine, L-glutamate and L-glutamine were also enriched in the obese microbiome. The mixed acid fermentation pathway and partial TCA cycle pathway (incorporate carbon from exogenous pyruvate, acetate, and glutamate into cellular amino acids) were also obesity-enriched pathways, suggesting that the capacities to ferment and utilize SCFAs were enhanced in the obese microbiome. In addition, the obesity-enriched pathways also contributed to ppGpp biosynthesis (regulate gene expression during the stringent response or other environmental stress in some bacteria) and polymyxin resistance (a part of antibiotic resistance). After FDR correction, the heathy-enrichment of GDP-mannose biosynthesis remained significant, while the obesity-enriched pathways including glucose and glucose-1-phosphate degradation, and biosynthesis of tetrahydrofolate, thiamin diphosphate, ubiquinol, L-glutamate, L-glutamine and ppGpp remained significant ($q < 0.25$).

Next, we compared pathway abundance between pre- vs. post-operative subjects (Fig. 5b). The pathways enriched in the pre-operative group also included 4 pathways responsible for the carbohydrate utilization. Twenty-two MetaCyc pathways increased after LSG (paired Wilcoxon signed-rank test; original $p < 0.05$, $q < 0.56$). Among these pathways, 11 were involved in nucleoside and nucleotide biosynthesis, suggesting that gut microbiome might be re-established after LSG. However, none of the enrichments were significant after FDR correction (all $q > 0.25$).

Using HUMAnN2, we also calculated pathway abundance based on contributions from individual species (Suppl. Table 6). We created species-specific pathway profiles, focusing on different pathways from the MetaCyc analyses of total community and the contributions of individual species. Comparison of healthy and obese microbial communities showed 58 different species contributions within 49 pathways (Wilcoxon rank sum test; original $p < 0.05$, $q < 0.28$), with 49 differences involving *E. coli*. Specifically, for two pathways enriched in the healthy group, the dominant coding species was *A. shahii* (original $p < 0.05$, $q < 0.16$), which was negatively correlated with VFA and WHR. Comparison of pre- and post-operative subjects showed 27 significant difference in 19 pathways. Interestingly, potential SCFA producer species *C. symbiosum*, *Clostridiales* bacterium *1 7 47FAA* and *C. asparagiforme* have significantly higher contributions to pathways responsible for the biosynthesis of adenosine nucleotides and guanosine deoxyribonucleotides as well as the degradation of sucrose and L-histidine in post-operative subjects.

2.5.2. Microbial pathways correlated with a panel of clinical characteristics

We combined the results from the significantly different MetaCyc pathways and important clinical characteristics for Spearman's correlation analyses (Spearman's correlation value >0.25 or <−0.25). Sixty-two samples combined from healthy controls and obese subjects were included. Heatmaps were constructed with Spearman's correlations (Fig. 6, Suppl. Table 7). It was surprising that BMI only had 7 correlations with pathways (original $p < 0.05$, $q < 0.41$), and none of the correlations remained significant after FDR correction. WHR (n = 64, original $p < 0.05$, $q < 0.07$), waist (n = 54, original $p < 0.05$, $q < 0.08$) and VFA (n = 53, original $p < 0.05$, $q < 0.09$) had much more frequent and significant correlations with pathways. The potentially protective SFA had 51 correlations with pathways (original $p < 0.05$, $q < 0.09$). Lower body fat was found to be protective against metabolic disorders [31], and the corresponding parameter hipline only had 12 correlations with pathways (original $p < 0.05$, $q < 0.24$). The results suggested that the obesity differentiated pathways might potentially contribute to adverse fat distribution. In order to evaluate the correlation strength of different obese parameters, we further compared the significant correlations between obese parameters and the obesity-related microbial pathways. Among the 6 obese parameters, VFA had strongest correlation coefficients, followed by WHR, BMI, SFA, waist and hipline (Suppl. Fig. 3). Pathways positively correlated with WHR, waist and VFA were involved in carbohydrate degradation and biosynthesis of L-phenylalanine, L-glutamate, L-glutamine, and lipopolysaccharides. These results indicated that the microbial functions in fermentation and utilization of carbohydrate, biosynthesis of L-glutamate and L-glutamine were closely related to visceral fat accumulation and abdominal obesity.

3. Discussion

Our metagenome-wide association study found that among the obese parameters, VFA had largest number of correlations with gut microbial species. Within the species negatively correlated with VFA, *E. eligens* had the strongest correlation, followed by *C. citroniae*, *C. symbiosum*, *B. uniformis*, *E. ventriosum*, *Ruminococcaceae bacterium D16*, *C. hathewayi*, *A. shahii* and *F. plautii*. After LSG, *C. symbiosum*, *C. hathewayi* and *C. citroniae*, were significantly increased. Microbial pathways involved in carbohydrate fermentation and biosynthesis of L-glutamate and L-glutamine might contribute to visceral fat accumulation.

The obesity-related metabolic and cardiovascular disease risks are closely related to fat distribution. The traditional anthropometric parameter BMI can only evaluate total body fat, but not fat distribution. The major fat depots in the human body include visceral fat, lower- and upper-body subcutaneous fat [25]. In this study, we measured 4 parameters of central obesity, including waist, WHR, VFA and SFA. Waist gauges both visceral fat and upper-body subcutaneous fat. WHR further combines waist and hipline, the latter represents the lower-body subcutaneous fat. Waist and WHR are all simple indices of central obesity. VFA and SFA measured by MRI can precisely distinguish visceral fat and upper-body subcutaneous fat. Different fat depots are significantly different in the uptake and release of fatty acid and secretion of adipokines and inflammation factors. Compared with subcutaneous fat, visceral fat is more active in storing dietary fatty acid [32], secreting adiponectin [33] and some inflammation cytokines like interleukin-6 [34], tumor necrosis factor-alpha [35] and colony-stimulating factor-1 [36]. Central obesity with excessive visceral fat accumulation significantly increased the risks of subclinical atherosclerosis [37], type 2 diabetes mellitus [38], cancer [39] and all-cause mortality [40]. Therefore, although the relationship between gut microbiota and obesity evaluated by BMI has been demonstrated before, it is essential to make further analysis on the relationships between gut microbiota and visceral fat.

Few studies have explored the relationships between gut microbiota and visceral fat. In the Twins UK cohort, Tim *et al.* performed 16S rRNA sequencing to determine correlations between visceral fat content detected by dual energy X-ray absorptiometry and the heritable components of gut microbiota [26]. They found that members of family *Ruminococcaceae*, *Lachnospiraceae* and genus *Oscillospira* were strongly related to visceral fat content. Most of the correlations were negative, which strongly supported our findings. In total, we found 6 species belonging to *Lachnospiraceae* (*C. citroniae*, *C. symbiosum*, *C. bolteae*, *C. asparagiforme*, *Lachnospiraceae bacterium 3 1 57FAA CT1*, and *C. nexile*) that were enriched in healthy controls or increased after LSG. Among them, *C. citroniae* and *C. symbiosum* were further negatively correlated

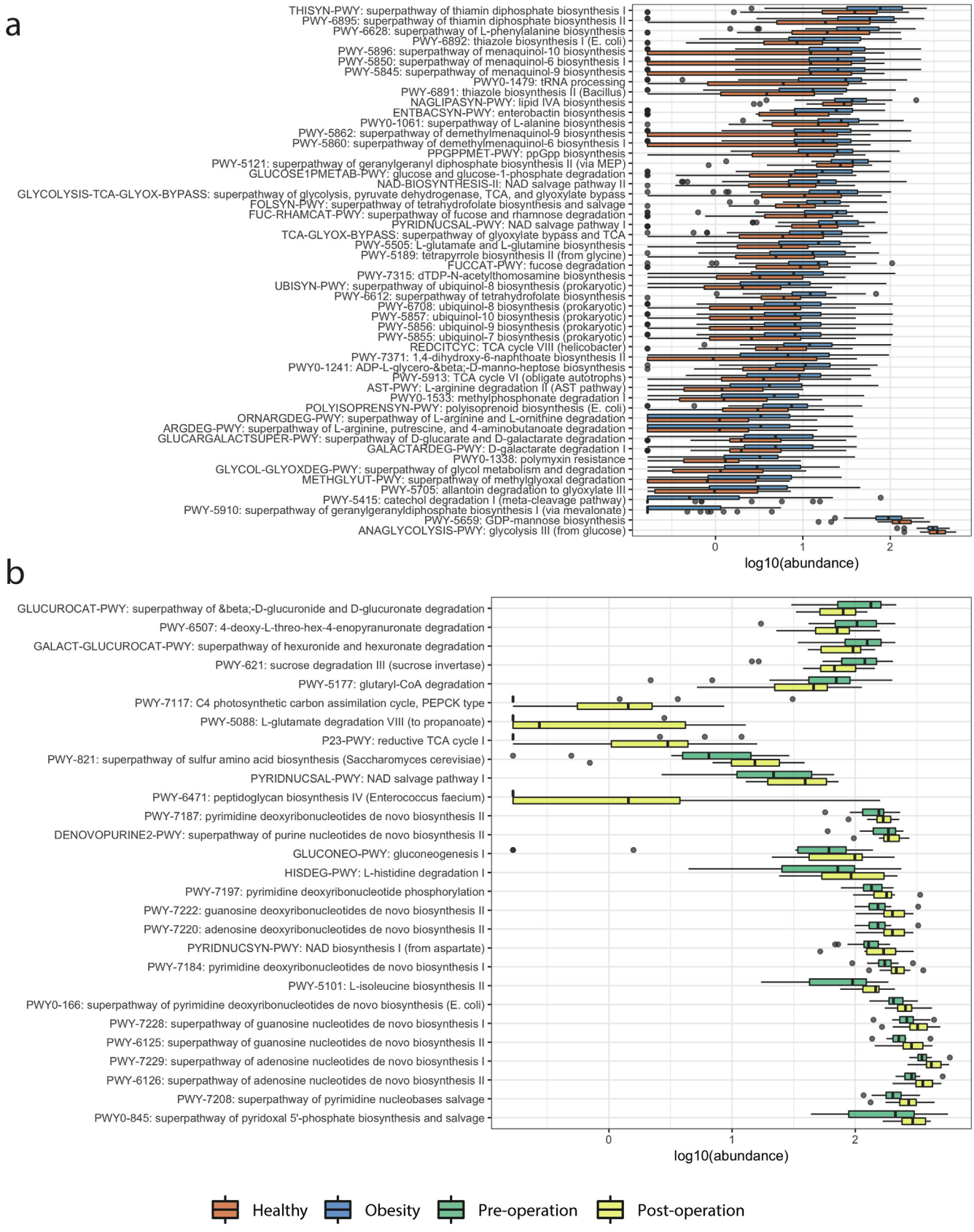

Fig. 5. Functional profiles of the gut microbiota in different participant groups. (a) MetaCyc pathways with different abundance between healthy controls and obese subjects (original $p < 0{\cdot}05$, $q < 0.30$, Wilcoxon rank sum test). Pathways with stars indicated $q < 0.25$. (b) MetaCyc pathways with different abundance between pre- vs. post-operative subjects (original $p < 0{\cdot}05$, $q < 0.56$, paired Wilcoxon signed-rank test).

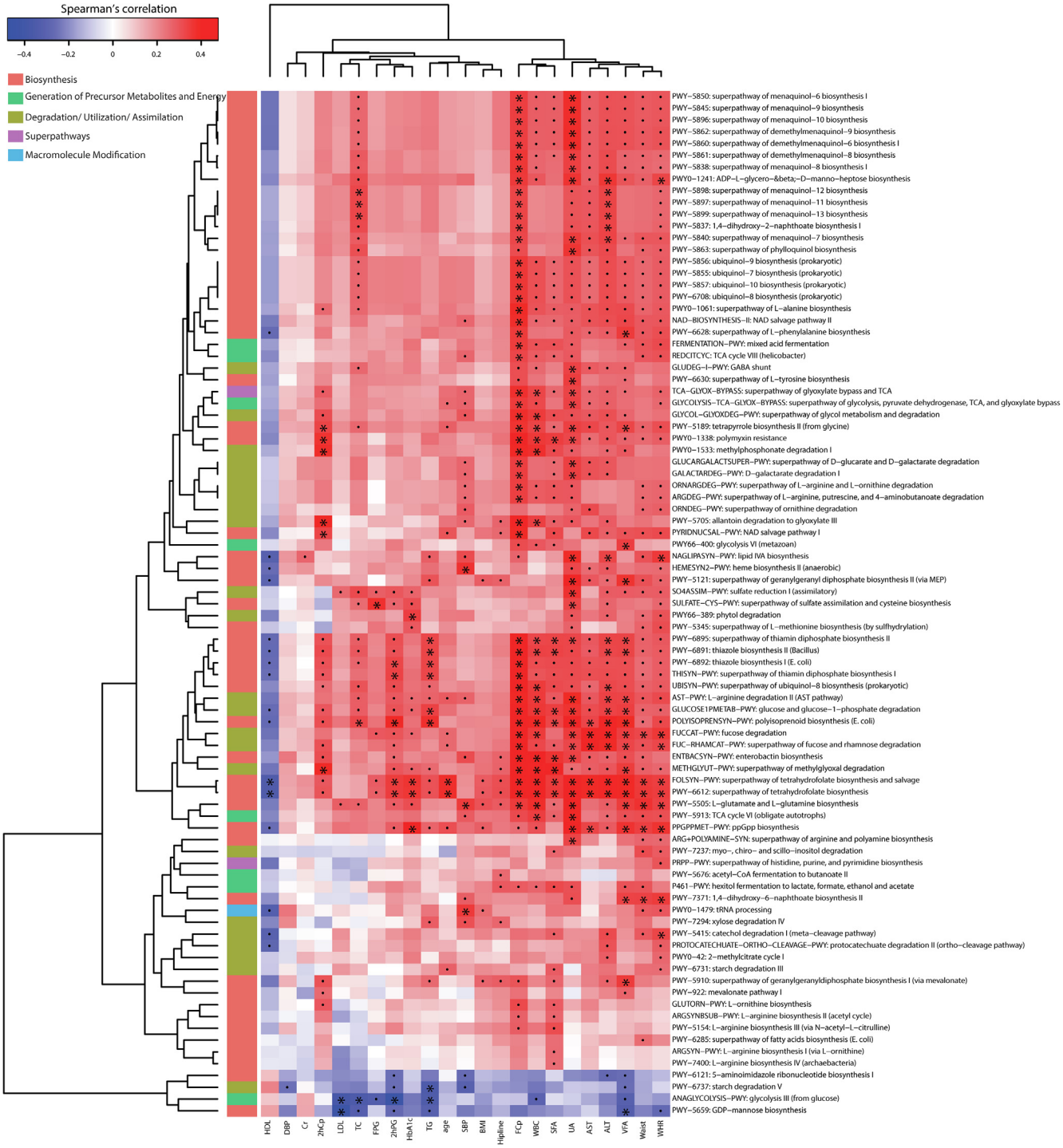

Fig. 6. Spearman's Correlation matrix for obesity-correlated pathways and clinical characteristics. MetaCyc pathways which were significantly correlated with 6 obese parameters were selected for performing correlation with clinical characteristics. Cell color indicated correlation type (red: positive, purple: negative). Cell with dot indicated original $p < 0.05$, cells with star indicated original $p < 0.01$ ($q < 0.26$). (For interpretation of the references to color in this figure legend, the reader is referred to the web version of this article.)

with VFA. We also found species belonging to *Ruminococcaceae* such as *F. plautii* and *R. bacterium D16* that were negatively correlated with VFA. Due to the lack of metagenomic data, the study of Tim *et al.* was limited in functional interpretation of the microbial dysbiosis. In our study, based on shotgun metagenomic data, we found that VFA had the strongest correlations with the obesity-differentiated species. We also found groups of microbial pathways which were positively correlated with visceral fat. Together, our study not only expanded the relationships between the gut microbiome and visceral fat at the species level, but also provided potential functional interpretation for the association between gut microbiota and visceral fat accumulation.

In another Chinese obesity cohort, Liu et al. also explored gut microbiome alterations among obese subjects and after LSG. In their study, obese parameters mainly included BMI, waist, WHR and whole body fat [11], while visceral fat was not measured. They

found that *D. longicatena* and *C. comes* were positively correlated with obesity, which was consistent with our findings. *B. thetaiotaomicron,* a healthy marker species which was negatively related to obese parameters in their study, was also increased after LSG in our study. However, we found that *D. longicatena* and *B. thetaiotaomicron* were not correlated with VFA. Consistent with their findings, we also found that the capacity of L-glutamate and L-glutamine biosynthesis was highly enriched in the obese microbiome. We further found that the capacity of L-glutamate and L-glutamine biosynthesis was positively correlated with VFA. After LSG, L-glutamate degradation pathway increased. L-glutamate is used to produce monosodium glutamate (MSG), a commonly used food additive that contributes to metabolic disorders [41–44]. Our results suggested that glutamate biosynthesis of gut microbiota might be an influencing factor of visceral fat accumulation.

We noted that a large group of *Clostridiales* might be considered as "good" microbes because they were enriched in healthy controls, increased after LSG, and were negatively correlated with metabolic disease markers. Previous studies suggested that *Clostridiales* were important in producing SCFAs [45–47]. Recent evidence suggested that SCFAs produced by gut microbiota exert multiple beneficial effects on the host energy metabolism [48]. *E. eligens*, which was negatively correlated with VFA in our study, is a SCFA producer in the healthy gut [17]. Jie et al. found that *E. eligens* was enriched in heathy individuals and decreased in atherosclerotic cardiovascular disease [16]. In a previous study investigating gut microbiota in malnourished Malawian children, *E. eligens* was a biomarker of mature gut microbiota [49]. Functionally, we found that pathways contributing to the fermentation and utilization of SCFAs were enhanced in the obese microbiome, which might lead to a relatively low level of SCFAs in the gut of obese subjects.

Bacterial metabolites (decomposition or biosynthesis) such as bile acids, SCFAs, and trimethylamine N-oxide are identified as essential mediators to construct the bidirectional association between gut microbiome and the host [4]. In our study, the main clues of the association mechanism between visceral fat accumulation and gut microbiome point to glutamate and SCFAs. In terms of glutamate, epidemiology studies found that dietary MSG intake contributed to increased risks of overweight [50,51]; in addition, circulating glutamate was positively associated with VFA, abdominal obesity, and insulin resistance [52,53]. In mice, MSG injection induced hypothalamic lesions, leptin resistance, and obesity [54,55]. Furthermore, MSG diet led to a significant increase in visceral fat accumulation and altered expression of many genes that were critical for adipocyte differentiation. Among them, Keratin-19 (a biomarker of visceral mesothelial cells) and cyclin D3 were significantly up-regulated, suggesting that MSG increased visceral adipocyte differentiation [56]. While in terms of SCFA, a previous study found that the SCFAs receptor G-protein coupled receptor 43 (GPR43) was a sensor of excessive dietary energy, inhibiting insulin signaling and fat accumulation in adipose tissue [57]. Propionate inhibited adipocytes formation from mesenchymal stem cells via GPR43 [58]. Fructo-oligosaccharides, a soluble dietary fiber, ameliorated visceral adiposity by increasing SCFAs production [59]. Moreover, dietary SCFAs were reported to induce a peroxisome proliferator-activated receptor-γ-dependent switch from lipid synthesis to utilization [60]. Generally, the potential mechanisms underlying the gut microbiome-glutamate/SCFAs-visceral fat accumulation link remains much for further exploration. The novel associations between specific bacterial species/pathways and visceral fat accumulation could provide new clues for microbiome-targeted therapies such as probiotics and FMT. Further studies investigating the targets and signaling pathways of glutamate and SCFAs in the host would promote the development of new drugs.

Our study has some limitations. Firstly, the sample size is relatively small. Secondly, that causality between the discovered species and VFA cannot be proven using our study design and should be further confirmed in germ-free mice. Thirdly, the study subjects are all Han Chinese, thus the results may not be generalized to other ethnic groups. Further clinical studies with larger prospective cohorts and multiethnic data are needed to fully elucidate the association between gut microbiome and visceral fat accumulation.

4. Conclusions

In this study, we established metagenomic associations between gut microbiome and visceral fat accumulation. VFA had the strongest correlation with the species that were differentially associated with obesity compared with other obese parameters, suggesting an intrinsic connection between the gut microbiome and metabolic cardiovascular diseases. Specific microbial species and pathways which were closely associated with visceral fat accumulation might lead to new therapies for metabolic disorders.

5. Materials and methods

5.1. Participants

From January 2017 to May 2018, 32 obese adults and 30 healthy participants aged 18 years or older were recruited at Shanghai Jiao Tong University Affiliated Sixth People's Hospital. Exclusion criteria were: malignant tumor, secondary obesity, acute inflammation, moderate to severe anemia, severe hepatic and renal dysfunction, heart failure, respiratory failure, gastrointestinal ulcers, inflammatory bowel disease, hyperthyroidism, hypothyroidism, subacute thyroiditis, schizophrenia, or hormone replacement therapy. For healthy controls, additional exclusion criteria were: BMI $\geq$ 24.00 kg/m^2, hypertension, history of obesity, impaired glucose tolerance, impaired fasting glucose, diabetes, or dyslipidemia. Fourteen out of 32 obese subjects underwent LSG and were followed for 6 months after surgery. LSG surgery was as described previously [61]. The clinical trials were registered in the Chinese Clinical Trial Registry (ChiCTR-COC-17011355, date of registration: 11 May 2017; ChiCTR-SOC-17011356, date of registration: 11 May 2017). All participants provided informed consent. The study was approved by the Ethics Committee of the Shanghai Jiao Tong University Affiliated Sixth People's Hospital and performed in accordance with the Helsinki declaration.

5.2. Anthropometric and laboratory assessments

Height and body weight were measured in subjects with light clothes and without hats or shoes. BMI was calculated as body weight in kilograms divided by height in meters squared. Waist was measured with a tape measure at the midaxillary line around the midpoint between the lower margin of the 12th rib and the iliac crest. Hipline was measured at the most prominent part of the buttocks. WHR was calculated as waist (cm) divided by hipline (cm). After 15 min of rest in a sitting position, blood pressure was measured at the right arm using an electronic sphygmomanometer.

Venous blood was drawn after a 10-hour overnight fast. The glucose oxidase method was used to detect fasting plasma glucose (FPG) and 2-hour plasma glucose (2hPG). FCp and 2-hour C-peptide (2hCp) were detected by radioimmunoassay (Beijing North Institute of Biological Technology, Beijing, China). HbA1c was detected by high performance liquid chromatography (Bio-Rad Laboratories, Hercules, CA, USA). Total cholesterol (TC), triglyceride

(TG), HDL, LDL, UA, creatinine (Cr), ALT and aspartate aminotransferase (AST) were detected by standard methods on a Hitachi 747 analyzer (Castle Hill, NSW, Australia). WBC was detected by nucleic acid staining on a XN-350 automated hematology analyzer (Sysmex Europe GmbH, Norderstedt, Germany).

5.3. Measurements of VFA and SFA

MRI is an internationally recognized method for precisely measuring abdominal fat [62]. MRI scanning was performed on all participants using a 3.0 T clinical MRI scanner (Archiva, Philips Medical System, Amsterdam, The Netherlands). MRI scans were obtained by T1 weighted sequence at the umbilicus level between L4 and L5 vertebrae in the supine position. The scanning thickness was 1 cm, the scanning field was 42 cm $\times$ 42 cm. Six layers were scanned. SliceOmatic software 4.2 (Tomovision, Montreal, Canada) was used to process images. Two trained observers analyzed the images independently. If the difference between their results was <10%, then took the averages as the recorded results. If the difference was larger than or equal to 10%, a third person who did not know the results would reanalyze the images and take the averages of the two results with a difference <10%.

5.4. Definitions

Obesity was defined as BMI $\geq$ 28.00 kg/m^2 [63].

5.5. Stool sample collection and DNA extraction

Before stool sample collection, all participants confirmed they did not take probiotics or yogurt in the past week and antibiotics in the past month. PSP Spin Stool DNA Plus Kits (Stratec Molecular GmbH, Berlin, Germany) were used for stool sample collection, storage, and DNA purification. About 150 mg of stool was collected in a stool collection tube with stool DNA stabilizer. Samples were kept at room temperature for up to 24 h and then transferred to −80℃. Bacterial DNA was extracted and purified according to the kit manual. A NanoDrop 2000 spectrophotometer was used in the preliminary testing for DNA quality and abundance. Qubit 2.0 fluorimeter (Thermo Fisher Scientific Inc., MA, USA) and agarose gel electrophoresis were further used to analyze the concentration, integrity, and purity of DNA samples.

5.6. Library preparation, metagenome sequencing and taxonomic profiling

A total amount of 700 ng DNA per sample was used as input material for the DNA sample preparations. Sequencing libraries were generated using NEB Next® Ultra DNA Library Prep Kit for Illumina® (NEB, USA). Index codes were added to attribute sequences to each sample. Briefly, AMPure XP system (Beckman Coulter, Beverly, USA) was used to purify the Chip DNA. After adenylation of 3′ ends of DNA fragments, the NEB Next Adaptor with hairpin loop structure were ligated to prepare for hybridization. Then electrophoresis was used to select DNA fragments specified in length. 3 μL USER Enzyme (NEB, USA) was used with size-selected, adaptor-ligated DNA at 37 °C for 15 min followed by 5 min at 95 °C before PCR. Then PCR was performed with Phusion High-Fidelity DNA polymerase, Universal PCR primers and Index (X) Primer. At last, PCR products were purified (AMPure XP system) and library quality was assessed on the Agilent Bioanalyzer 2100 system. After the cBOT cluster is generated, the library preparations were sequenced on an Illumina Novaseq 6000 platform and 150 bp paired-end reads were generated. Raw sequencing paired-end reads passed through standard quality control measures after human contamination, adapter regions, and low-quality reads were removed, as per Li et al. [64,65].

Taxonomic classification and quantification were performed using MetaPhlAn2 with default settings [66]. Relative abundances of taxa were extracted from original outputs for each taxonomic level. Prokaryotic community profiles were constructed at the phylum, family, genus, and species levels for statistical analyses.

5.7. Microbial community composition

Alpha diversity indices detailing microbial community composition within samples were calculated using vegan [67] in R. Shannon index was used for alpha diversity evaluation based on the relative abundance of each taxonomic level. Statistical comparisons of healthy controls vs. obese subjects and pre- vs. post-operative subjects were performed by Wilcoxon rank sum test and rank sum test paired Wilcoxon signed-rank test. For estimating community dissimilarities, Bray-Curtis distances were calculated by phyloseq [68] and vegan [67] and Aitchison distances were calculated by robCompositions [69] based on the relative abundance of each taxon at phylum, family, genus and species level. Adonis from vegan package [67] in R was used for PERMANOVA tests to evaluate differences among groups (number of permutation set to 999). Within-group distance (Bray-Curtis distance among samples from the same group) indicating the community divergence and between-group distances (Bray-Curtis distance among samples from each of the two groups) indicating the difference between two communities were determined and compared by Wilcoxon rank sum test, paired Wilcoxon signed-rank and Kruskal-Wallis tests, where appropriate.

5.8. Species comparisons

Species were filtered by 10% prevalence across all samples and the relative abundances of remaining species were used for statistical comparisons of healthy controls vs. obese subjects and pre- vs. post-operative subjects by Wilcoxon rank sum test and paired Wilcoxon signed-rank tests, respectively. The Benjamini-Hochberg FDR correction [70] was applied to adjust p values for multiple tests in R. CoDA were further performed for statistical test for the significant result with the ALDEx2 package in R [71]. Datasets were first transformed based on centered log-ratio (clr). Wilcoxon rank sum test for comparisons between healthy controls and obese subjects and paired Wilcoxon signed-rank tests between pre- and post-operative subjects were performed. Expected p value and expected Benjamini-Hochberg corrected p value were used for significance evaluation.

5.9. Correlation analyses using clinical metadata abundance

To evaluate the potential effects of the gut microbiome on obese parameters, we calculated Spearman's correlations between species abundance and 24 clinical characteristics relevant to obesity. FDR correction was applied to each obese parameter across species.

5.10. Co-abundance networks

Co-abundance networks were created using BAnOCC based on prevalent species (in over 20% of participants) within microbial communities in four participant groups for comparisons (healthy controls vs. obese subjects and pre- vs post-operative subjects) [72]. BAnOCC was executed with 5 chains, 5000 iterations, and 1000 warmup cycles to read convergence. For posterior inference, we used a 95% credible interval. Only significant correlations with an absolute estimated coefficient of at least 30% were used for fur-

ther analyses of obese and healthy communities. We increased the absolute estimated coefficient to 60% for pre- and post-operative communities, for illustration purpose.

5.11. Functional annotation

HUMAnN2 [73] was used with metagenomic reads to estimate gene family abundances. Reads per kilobase (RPK) values for gene family abundances were copies per million (CPM) normalized. MetaCyc pathway and species-coding pathway profiles were further annotated. Functional alpha based on MetaCyc pathway profiles were analyzed with Wilcoxon rank sum test and paired Wilcoxon signed-rank tests as for taxonomic profiles. Wilcoxon rank sum tests were detecting statistically significantly different MetaCyc pathway and species-coding pathways among groups. Spearman's correlations were determined between significant pathways and important clinical characteristics. The absolute coefficient values from the significant correlations of the 6 obese parameters were selected and compared by using Wilcoxon rank sum tests.

5.12. Data visualization

Packages ggplot2 and gplots in R and matplotlib in Python were used for visualizations. Cytoscape v3.7.1 was used for co-abundance network and correlation visualization.

Ethics approval and consent to participate

All participants provided informed consent. The study was approved by the Ethics Committee of the Shanghai Jiao Tong University Affiliated Sixth People's Hospital and performed in accordance with the Helsinki declaration. Clinical trials were registered in the Chinese Clinical Trial Registry (ChiCTR-COC-17011355; ChiCTR-SOC-17011356).

Availability of data and material

The metagenome sequencing data supporting the conclusions of this article is available in the Sequence Read Archive data repository with accession number PRJNA597839. The clinical data supporting our results of this article is included within the article (Suppl. Table 8).

Author agreement

All authors have seen and approved the final version of the manuscript being submitted. The manuscript is not under consideration for publication elsewhere. Its publication is approved by all authors and by the responsible authorities where the work was carried out. If the manuscript is accepted, it will not be published elsewhere in the same form, in English or in any other language, including electronically without the written consent of the copyright holder.

Funding

This work was funded by the National Key R&D Program of China (2016YFA0502003).

CRediT authorship contribution statement

Xiaomin Nie: Formal analysis, Investigation, Writing - original draft. **Jiarui Chen:** Formal analysis, Writing - original draft, Visualization. **Xiaojing Ma:** Investigation, Resources. **Yueqiong Ni:** Formal analysis, Methodology. **Yun Shen:** Investigation. **Haoyong Yu:** Conceptualization, Data curation, Resources, Writing - review & editing. **Gianni Panagiotou:** Conceptualization, Supervision, Methodology, Data curation, Writing - review & editing. **Yuqian Bao:** Conceptualization, Supervision, Data curation, Funding acquisition, Writing - review & editing.

Declaration of Competing Interest

The authors declare that they have no known competing financial interests or personal relationships that could have appeared to influence the work reported in this paper.

Acknowledgement

We thank the supports of Biobank of Shanghai Jiao Tong University Affiliated Sixth People's Hospital.

Appendix A. Supplementary data

Supplementary data to this article can be found online at https://doi.org/10.1016/j.csbj.2020.09.026.

References

[1] Savage DC. Microbial ecology of the gastrointestinal tract. Annu Rev Microbiol 1977;31:107–33. https://doi.org/10.1146/annurev.mi.31.100177.000543.
[2] Zhao L. The gut microbiota and obesity: from correlation to causality. Nat Rev Microbiol 2013;11:639–47. https://doi.org/10.1038/nrmicro3089.
[3] Maruvada P, Leone V, Kaplan LM, Chang EB. The human microbiome and obesity: moving beyond associations. Cell Host Microbe 2017;22:589–99. https://doi.org/10.1016/j.chom.2017.10.005.
[4] Bouter KE, van Raalte DH, Groen AK, Nieuwdorp M. Role of the gut microbiome in the pathogenesis of obesity and obesity-related metabolic dysfunction. Gastroenterology 2017;152:1671–8. https://doi.org/10.1053/j.gastro.2016.12.048.
[5] Ley RE, Backhed F, Turnbaugh P, Lozupone CA, Knight RD, et al. Obesity alters gut microbial ecology. Proc Natl Acad Sci U S A 2005;102:11070–5. https://doi.org/10.1073/pnas.0504978102.
[6] Duncan SH, Lobley GE, Holtrop G, Ince J, Johnstone AM, et al. Human colonic microbiota associated with diet, obesity and weight loss. Int J Obes 2008;32:1720–4. https://doi.org/10.1038/ijo.2008.155.
[7] Schwiertz A, Taras D, Schafer K, Beijer S, Bos NA, et al. Microbiota and SCFA in lean and overweight healthy subjects. Obesity (Silver Spring) 2010;18:190–5. https://doi.org/10.1038/oby.2009.167.
[8] Turnbaugh PJ, Backhed F, Fulton L, Gordon JI. Diet-induced obesity is linked to marked but reversible alterations in the mouse distal gut microbiome. Cell Host Microbe 2008;3:213–23. https://doi.org/10.1016/j.chom.2008.02.015.
[9] Ziętak M, Kovatcheva-Datchary P, Markiewicz LH, Ståhlman M, Kozak LP, et al. Altered microbiota contributes to reduced diet-induced obesity upon cold exposure. Cell Metab 2016;23:1216–23. https://doi.org/10.1016/j.cmet.2016.05.001.
[10] Parséus A, Sommer N, Sommer F, Caesar R, Molinaro A, et al. Microbiota-induced obesity requires farnesoid X receptor. Gut 2017;66:429–37. https://doi.org/10.1136/gutjnl-2015-310283.
[11] Liu R, Hong J, Xu X, Feng Q, Zhang D, et al. Gut microbiome and serum metabolome alterations in obesity and after weight-loss intervention. Nat Med 2017;23:859–68. https://doi.org/10.1038/nm.4358.
[12] Plovier H, Everard A, Druart C, Depommier C, Van Hul M, et al. A purified membrane protein from Akkermansia muciniphila or the pasteurized bacterium improves metabolism in obese and diabetic mice. Nat Med 2017;23:107–13. https://doi.org/10.1038/nm.4236.
[13] Simon MC, Strassburger K, Nowotny B, Kolb H, Nowotny P, et al. Intake of Lactobacillus reuteri improves incretin and insulin secretion in glucose-tolerant humans: a proof of concept. Diabetes Care 2015;38:1827–34. https://doi.org/10.2337/dc14-2690.
[14] Wang J, Jia H. Metagenome-wide association studies: fine-mining the microbiome. Nat Rev Microbiol 2016;14:508–22. https://doi.org/10.1038/nrmicro.2016.83.
[15] Qin J, Li Y, Cai Z, Li S, Zhu J, et al. A metagenome-wide association study of gut microbiota in type 2 diabetes. Nature 2012;490:55–60. https://doi.org/10.1038/nature11450.
[16] Jie Z, Xia H, Zhong SL, Feng Q, Li S, et al. The gut microbiome in atherosclerotic cardiovascular disease. Nat Commun 2017;8:845. https://doi.org/10.1038/s41467-017-00900-1.
[17] Zhao L, Zhang F. Gut bacteria selectively promoted by dietary fibers alleviate type 2 diabetes. Science 2018;359:1151–6. https://doi.org/10.1126/science.aao5774.

[18] Le Chatelier E, Nielsen T, Qin J, Prifti E, Hildebrand F, et al. Richness of human gut microbiome correlates with metabolic markers. Nature 2013;500:541–6. https://doi.org/10.1038/nature12506.
[19] Piche ME, Poirier P, Lemieux I, Despres JP. Overview of epidemiology and contribution of obesity and body fat distribution to cardiovascular disease: an update. Prog Cardiovasc Dis 2018;61:103–13. https://doi.org/10.1016/j.pcad.2018.06.004.
[20] Chau YY, Bandiera R, Serrels A, Martinez-Estrada OM, Qing W, et al. Visceral and subcutaneous fat have different origins and evidence supports a mesothelial source. Nat Cell Biol 2014;16:367–75. https://doi.org/10.1038/ncb2922.
[21] Wander PL, Boyko EJ, Leonetti DL, McNeely MJ, Kahn SE, et al. Change in visceral adiposity independently predicts a greater risk of developing type 2 diabetes over 10 years in Japanese Americans. Diabetes Care 2013;36:289–93. https://doi.org/10.2337/dc12-0198.
[22] Abraham TM, Pedley A, Massaro JM, Hoffmann U, Fox CS. Association between visceral and subcutaneous adipose depots and incident cardiovascular disease risk factors. Circulation 2015;132:1639–47. https://doi.org/10.1161/circulationaha.114.015000.
[23] Britton KA, Massaro JM, Murabito JM, Kreger BE, Hoffmann U, et al. Body fat distribution, incident cardiovascular disease, cancer, and all-cause mortality. J Am Coll Cardiol 2013;62:921–5. https://doi.org/10.1016/j.jacc.2013.06.027.
[24] Zhang C, Rexrode KM, van Dam RM, Li TY, Hu FB. Abdominal obesity and the risk of all-cause, cardiovascular, and cancer mortality: sixteen years of follow-up in US women. Circulation 2008;117:1658–67. https://doi.org/10.1161/circulationaha.107.739714.
[25] Tchkonia T, Thomou T, Zhu Y, Karagiannides I, Pothoulakis C, et al. Mechanisms and metabolic implications of regional differences among fat depots. Cell Metab 2013;17:644–56. https://doi.org/10.1016/j.cmet.2013.03.008.
[26] Beaumont M, Goodrich JK, Jackson MA, Yet I, Davenport ER, et al. Heritable components of the human fecal microbiome are associated with visceral fat. Genome Biol 2016;17:189. https://doi.org/10.1186/s13059-016-1052-7.
[27] Goffredo M, Mass K, Parks EJ, Wagner DA, McClure EA, et al. Role of gut microbiota and short chain fatty acids in modulating energy harvest and fat partitioning in youth. J Clin Endocrinol Metab 2016;101:4367–76. https://doi.org/10.1210/jc.2016-1797.
[28] Le Roy CI, Bowyer RCE. Dissecting the role of the gut microbiota and diet on visceral fat mass accumulation. Sci Rep 2019;9:9758. https://doi.org/10.1038/s41598-019-46193-w.
[29] Delday M, Mulder I, Logan ET, Grant G. Bacteroides thetaiotaomicron ameliorates colon inflammation in preclinical models of Crohn's disease. Inflamm Bowel Dis 2019;25:85–96. https://doi.org/10.1093/ibd/izy281.
[30] Park JE, Park SY, Song DJ, Huh HJ, Ki CS, et al. A case of Bacteroides pyogenes bacteremia secondary to liver abscess. Anaerobe 2016;42:78–80. https://doi.org/10.1016/j.anaerobe.2016.09.002.
[31] Vasan SK, Osmond C, Canoy D. Comparison of regional fat measurements by dual-energy X-ray absorptiometry and conventional anthropometry and their association with markers of diabetes and cardiovascular disease risk. Int J Obes 2018;42:850–7. https://doi.org/10.1038/ijo.2017.289.
[32] Jensen MD, Sarr MG, Dumesic DA, Southorn PA, Levine JA. Regional uptake of meal fatty acids in humans. Am J Physiol Endocrinol Metab 2003;285:E1282–8. https://doi.org/10.1152/ajpendo.00220.2003.
[33] Kovacova Z, Tencerova M, Roussel B, Wedellova Z, Rossmeislova L, et al. The impact of obesity on secretion of adiponectin multimeric isoforms differs in visceral and subcutaneous adipose tissue. Int J Obes 2012;36:1360–5. https://doi.org/10.1038/ijo.2011.223.
[34] Fontana L, Eagon JC, Trujillo ME, Scherer PE, Klein S. Visceral fat adipokine secretion is associated with systemic inflammation in obese humans. Diabetes 2007;56:1010–3. https://doi.org/10.2337/db06-1656.
[35] Cartier A, Lemieux I, Alméras N, Tremblay A, Bergeron J, et al. Visceral obesity and plasma glucose-insulin homeostasis: contributions of interleukin-6 and tumor necrosis factor-alpha in men. J Clin Endocrinol Metab 2008;93:1931–8. https://doi.org/10.1210/jc.2007-2191.
[36] Harman-Boehm I, Blüher M, Redel H, Sion-Vardy N, Ovadia S, et al. Macrophage infiltration into omental versus subcutaneous fat across different populations: effect of regional adiposity and the comorbidities of obesity. J Clin Endocrinol Metab 2007;92:2240–7. https://doi.org/10.1210/jc.2006-1811.
[37] Wang Y, Ma X, Zhou M, Zong W, Zhang L, et al. Contribution of visceral fat accumulation to carotid intima-media thickness in a Chinese population. Int J Obes 2012;36:1203–8. https://doi.org/10.1038/ijo.2011.222.
[38] Huang T, Qi Q, Zheng Y, Ley SH, Manson JE, et al. Genetic predisposition to central obesity and risk of type 2 diabetes: two independent cohort studies. Diabetes Care 2015;38:1306–11. https://doi.org/10.2337/dc14-3084.
[39] Barberio AM, Alareeki A, Viner B, Pader J, Vena JE, et al. Central body fatness is a stronger predictor of cancer risk than overall body size. Nat Commun 2019;10:383-. https://doi.org/10.1038/s41467-018-08159-w.
[40] Tsujimoto T, Kajio H. Abdominal obesity is associated with an increased risk of all-cause mortality in patients with HFpEF. J Am Coll Cardiol 2017;70:2739–49. https://doi.org/10.1016/j.jacc.2017.09.1111.
[41] Majewski M, Jurgonski A, Fotschki B, Juskiewicz J. The toxic effects of monosodium glutamate (MSG) - The involvement of nitric oxide, prostanoids and potassium channels in the reactivity of thoracic arteries in MSG-obese rats. Toxicol Appl Pharmacol 2018;359:62–9. https://doi.org/10.1016/j.taap.2018.09.016.
[42] Hernandez Bautista RJ, Mahmoud AM, Konigsberg M, Lopez Diaz Guerrero NE. Obesity: Pathophysiology, monosodium glutamate-induced model and anti-obesity medicinal plants. Biomed Pharmacother 2019;111:503–16. https://doi.org/10.1016/j.biopha.2018.12.108.
[43] Bahadoran Z, Mirmiran P, Ghasemi A. Monosodium glutamate (MSG)-induced animal model of type 2 diabetes. Methods Mol Biol 2019;1916:49–65. https://doi.org/10.1007/978-1-4939-8994-2_3.
[44] Sasaki Y, Suzuki W, Shimada T, Iizuka S, Nakamura S, et al. Dose dependent development of diabetes mellitus and non-alcoholic steatohepatitis in monosodium glutamate-induced obese mice. Life Sci 2009;85:490–8. https://doi.org/10.1016/j.lfs.2009.07.017.
[45] Tanca A, Palomba A, Fraumene C, Manghina V, Silverman M, et al. Clostridial butyrate biosynthesis enzymes are significantly depleted in the gut microbiota of nonobese diabetic mice. mSphere 2018;3:e00492–e518. https://doi.org/10.1128/mSphere.00492-18.
[46] Zhang D, Fu X, Dai X, Chen Y, Dai L. A new biological process for short-chain fatty acid generation from waste activated sludge improved by Clostridiales enhancement. Environ Sci Pollut Res Int 2016;23:23972–82. https://doi.org/10.1007/s11356-016-7579-z.
[47] Gargari G, Taverniti V, Gardana C, Cremon C, Canducci F, et al. Fecal Clostridiales distribution and short-chain fatty acids reflect bowel habits in irritable bowel syndrome. Environ Microbiol 2018;20:3201–13. https://doi.org/10.1111/1462-2920.14271.
[48] Kasubuchi M, Hasegawa S, Hiramatsu T, Ichimura A, Kimura I. Dietary gut microbial metabolites, short-chain fatty acids, and host metabolic regulation. Nutrients 2015;7:2839–49. https://doi.org/10.3390/nu7042839.
[49] Blanton LV, Charbonneau MR, Salih T, Barratt MJ, Venkatesh S, et al. Gut bacteria that prevent growth impairments transmitted by microbiota from malnourished children. Science 2016;351:6275. https://doi.org/10.1126/science.aad3311.
[50] He K, Zhao L, Daviglus ML, Dyer AR, Van Horn L, et al. Association of monosodium glutamate intake with overweight in Chinese adults: the INTERMAP Study. Obesity (Silver Spring) 2008;16:1875–80. https://doi.org/10.1038/oby.2008.274.
[51] He K, Du S, Xun P, Sharma S, Wang H, et al. Consumption of monosodium glutamate in relation to incidence of overweight in Chinese adults: China Health and Nutrition Survey (CHNS). Am J Clin Nutr 2011;93:1328–36. https://doi.org/10.3945/ajcn.110.008870.
[52] Takashina C, Tsujino I, Watanabe T, Sakaue S, Ikeda D, et al. Associations among the plasma amino acid profile, obesity, and glucose metabolism in Japanese adults with normal glucose tolerance. Nutr Metab (Lond) 2016;13:5. https://doi.org/10.1186/s12986-015-0059-5.
[53] Maltais-Payette I, Allam-Ndoul B, Pérusse L, Vohl MC, Tchernof A. Circulating glutamate level as a potential biomarker for abdominal obesity and metabolic risk. Nutr Metab Cardiovasc Dis 2019;29:1353–60. https://doi.org/10.1016/j.numecd.2019.08.015.
[54] Olney JW. Brain lesions, obesity, and other disturbances in mice treated with monosodium glutamate. Science 1969;164:719–21. https://doi.org/10.1126/science.164.3880.719.
[55] Matysková R, Maletínská L, Maixnerová J, Pirník Z, Kiss A, et al. Comparison of the obesity phenotypes related to monosodium glutamate effect on arcuate nucleus and/or the high fat diet feeding in C57BL/6 and NMRI mice. Physiol Res 2008;57:727–34.
[56] Collison KS, Maqbool ZM, Inglis AL, Makhoul NJ, Saleh SM, et al. Effect of dietary monosodium glutamate on HFCS-induced hepatic steatosis: expression profiles in the liver and visceral fat. Obesity (Silver Spring) 2010;18:1122–34. https://doi.org/10.1038/oby.2009.502.
[57] Kimura I, Ozawa K, Inoue D, Imamura T, Kimura K, et al. The gut microbiota suppresses insulin-mediated fat accumulation via the short-chain fatty acid receptor GPR43. Nat Commun 2013;4:1829. https://doi.org/10.1038/ncomms2852.
[58] Iván J, Major E, Sipos A, Kovács K, Horváth D, et al. The short-chain fatty acid propionate inhibits adipogenic differentiation of human chorion-derived mesenchymal stem cells through the free fatty acid receptor 2. Stem Cells Dev 2017;26:1724–33. https://doi.org/10.1089/scd.2017.0035.
[59] Takai A, Kikuchi K, Ichimura M, Tsuneyama K, Moritoki Y, et al. Fructo-oligosaccharides ameliorate steatohepatitis, visceral adiposity, and associated chronic inflammation via increased production of short-chain fatty acids in a mouse model of non-alcoholic steatohepatitis. BMC Gastroenterol 2020;20:46. https://doi.org/10.1186/s12876-020-01194-2.
[60] den Besten G, Bleeker A, Gerding A, van Eunen K, Havinga R, et al. Short-chain fatty acids protect against high-fat diet-induced obesity via a PPARγ-dependent switch from lipogenesis to fat oxidation. Diabetes 2015;64:2398–408. https://doi.org/10.2337/db14-1213.
[61] Di J, Wang C, Zhang P, Han X, Liu W, et al. The middle-term result of laparoscopic sleeve gastrectomy in Chinese obesity patients in a single hospital, with the review of literatures and strategy for gastric stenosis. Ann Transl Med 2018;6:479. https://doi.org/10.21037/atm.2018.12.28.
[62] Alberti KG, Zimmet P, Shaw J. Metabolic syndrome–a new world-wide definition. A Consensus Statement from the International Diabetes Federation. Diabet Med 2006;23:469–80. https://doi.org/10.1111/j.1464-5491.2006.01858.x.
[63] Chen C, Lu FC, Department of Disease Control Ministry of Health PRC. The guidelines for prevention and control of overweight and obesity in Chinese adults. Biomed Environ Sci 2004;17(Suppl):1–36.

[64] Li J, Sung CY, Lee N, Ni Y, Pihlajamaki J, et al. Probiotics modulated gut microbiota suppresses hepatocellular carcinoma growth in mice. Proc Natl Acad Sci U S A 2016;113:E1306–15. https://doi.org/10.1073/pnas.1518189113.
[65] Li J, Rettedal EA, van der Helm E, Ellabaan M, Panagiotou G, et al. Antibiotic treatment drives the diversification of the human gut resistome. Genom Proteom Bioinf 2019;17:39–51. https://doi.org/10.1016/j.gpb.2018.12.003.
[66] Segata N, Waldron L, Ballarini A, Narasimhan V, Jousson O, et al. Metagenomic microbial community profiling using unique clade-specific marker genes. Nat Methods 2012;9:811–4. https://doi.org/10.1038/nmeth.2066.
[67] P D (2013) VEGAN, a package of R functions for community ecology. J Veg Sci 14:4.
[68] McMurdie PJ, Holmes S. phyloseq: an R package for reproducible interactive analysis and graphics of microbiome census data. PLoS ONE 2013;8:. https://doi.org/10.1371/journal.pone.0061217e61217.
[69] Templ M, Hron K, Filzmoser P. robCompositions: An R-package for Robust Statistical Analysis of Compositional Data. John Wiley & Sons, Ltd; 2011.
[70] Benjamini YHY. Controlling the false discovery rate: a practical and powerful approach to multiple testing. J R Stat Soc Ser B Methodol 1995;57:12.
[71] Fernandes AD, Macklaim JM, Linn TG, Reid G, Gloor GB. ANOVA-like differential expression (ALDEx) analysis for mixed population RNA-Seq. PLoS ONE 2013;8:. https://doi.org/10.1371/journal.pone.0067019e67019.
[72] Schwager E, Mallick H. A Bayesian method for detecting pairwise associations in compositional data. PLoS Comput Biol 2017;13:. https://doi.org/10.1371/journal.pcbi.1005852e1005852.
[73] Franzosa EA, McIver LJ, Rahnavard G. Species-level functional profiling of metagenomes and metatranscriptomes. Nat Meth 2018;15:962–8. https://doi.org/10.1038/s41592-018-0176-y.